

Solid electrolytes based on lithium-containing lanthanum metaniobates

A. Belous*, E. Pashkova, O. Gavrilenko, O. V'yunov, L. Kovalenko

V.I. Vernadskii, Institute of General & Inorganic Chemistry, Kyiv, Ukraine

Abstract

The structure and transport properties of lithium-containing lanthanum metaniobates with defect-perovskite structure, $\text{La}_{2/3-x}\text{Li}_{3x}\square_{4/3-2x}\text{Nb}_2\text{O}_6$, have been studied. It has been shown that in the structure of $\text{La}_{2/3-x}\text{Li}_{3x}\square_{4/3-2x}\text{Nb}_2\text{O}_6$, Li^+ cations occupy, preferably, positions 1a in the range $x=0\text{--}\approx 0.5$, and occupy positions 1c (vacancies) at $x>0.5$. It has been noted that the direction $1c \leftrightarrow 1c$ is energetically a more favorable pathway of lithium ion migration. It has been shown that the materials under investigation possess a high lithium ion-conductivity.

© 2003 Elsevier Ltd. All rights reserved.

Keywords: Ionic conductivity; Niobates; Powders-solid state reaction; Rietveld analysis; X-ray methods

1. Introduction

The interest in lithium-containing lanthanum metaniobates $\text{La}_{2/3-x}\text{Li}_{3x}\square_{4/3-2x}\text{Nb}_2\text{O}_6$ (where \square is vacancy in lanthanum site) is due to the possibility of obtaining on their basis lithium-conducting solid electrolytes.¹ We proposed for the first time an unconventional approach to the search for and synthesis of novel cation-conducting materials, which consists of the introduction of ions into a basic structure which is potentially convenient for charge transport.² We have prepared solid electrolytes with high lithium ion-conductivity by the aliovalent of 3Li^+ for La^{3+} in the structure of the defect perovskite $\text{La}_{2/3}\square_{1/3}\text{TiO}_3$.² The fact that complex oxides $\text{La}_{2/3-x}\text{Li}_{3x}\square_{4/3-2x}\text{Nb}_2\text{O}_6$ have promise in the development of lithium-conducting materials on their basis is associated with the peculiarities of the crystal lattice of the lanthanum metaniobate $\text{La}_{2/3}\square_{4/3}\text{Nb}_2\text{O}_6$ with defect-perovskite structure (Fig. 1).³ The presence in the structure of a sufficient number of vacancies and channels, where lithium ions can reside, creates prerequisites for lithium ion-conduction.

The aim of the present work was to study crystallographic features and electrophysical properties of lithium-

containing lanthanum metaniobates with defect-perovskite structure, $\text{La}_{2/3-x}\text{Li}_{3x}\square_{4/3-2x}\text{Nb}_2\text{O}_6$ at $x=0\text{--}0.616$.

2. Experimental

The compounds were synthesized using solid-state reactions technique. Extra pure Li_2CO_3 , Nb_2O_5 and La_2O_3 of the sort “LO-1” were used as starting reagents. To remove moisture and adsorbed gases, heat treatments of the reagents were made for 2 h at 570 K (Li_2CO_3), 1020 K (Nb_2O_5) and 1220 K (La_2O_3). Taking into account the high hygroscopicity of the starting components and the ability of La_2O_3 to actively absorb CO_2 from air, the reagents were weighed just after heat treatment. Homogenizing grinding was performed in a vibrating mill in acetone for 5 h. The blend was evaporated, dried additionally at 370 K (1 h), and sieved through a nylon net (0.063 mm). Powders were pressed into tablets ($d=10$ mm) under a pressure of 500 kPa and synthesized at 1320 K (2 h) in a furnace with heaters made of silicon carbide. Samples had been ground, homogenized in a vibrating mill and dried. A 5% aqueous solution of polyvinyl alcohol was added as plasticizer. The pressed samples were sintered at 1400–1520 K (1 h).

The phases were identified by X-ray powder diffractograms (XRPD) taken on a DRON-4-07 diffractometer

* Corresponding author. Tel.: +380-44-42-211; fax: +380-44-44-42-211.

E-mail address: belous@mail.kar.net (A. Belous).

(Cu $K\alpha$ radiation; 40 kV, 18 mA). Data were collected in the range $2\theta = 10$ – 150° in step mode with the step $\Delta 2\theta = 0.02^\circ$ and an exposure time of 6 sec each point. SiO_2 (2θ standard) and NIST SRM1976- Al_2O_3 (certified intensity standard) were used as external standards.⁴ The crystal parameters were refined using Rietveld full-profile analysis (FullProf program, version 3.5d).

The electrical properties were measured on a PGSTAT-30 impedance analyzer (Solartron) in a frequency range of 10 Hz–1 MHz. Silver applied to samples by thermochemical method was used as electrodes. Samples ca. 9 mm in diameter and ca. 3 mm in thickness were used for measurements. The equivalent circuit was determined using the computer program Frequency Response Analyzer 4.7.

3. Results and discussion

XRPD of $\text{La}_{2/3-x}\text{Li}_{3x}\square_{4/3-2x}\text{Nb}_2\text{O}_6$ samples with various amount of Li (x) at $x < 0.25$ indicates the formation of single-phase products with defect-perovskite structure of orthorhombic crystal system (space group Pmmm). At $x > 0.25$, when the relation $[\text{Li}^+]/[\square] > 1$ (where $[\text{Li}^+]$ and $[\square]$ are the number of lithium ions and vacancies respectively) holds, a lithium metaniobate (LiNbO_3) phase with pseudoilmenite structure (space group R3c) is present in addition to the perovskite phase. The amount of LiNbO_3 increases with x , and it is

predominant at $x = 0.47$ and becomes the main phase at $x = 0.62$. The presence of superstructure reflections in diffractograms of $\text{La}_{2/3}\square_{4/3}\text{Nb}_2\text{O}_6$ indicates ordering of lattice vacancies,^{5,6} whereas their broadening as well as the decrease in their intensity with increasing amount of lithium (x) indicate statistical occupation of vacant sites and a decrease in the degree of order.

Structure parameters of complex oxides $\text{La}_{2/3-x}\text{Li}_{3x}\square_{4/3-2x}\text{Nb}_2\text{O}_6$ as a function of lithium content are given in the table. The atomic coordinates in the structure of $\text{La}_{2/3}\square_{4/3}\text{Nb}_2\text{O}_6$ were taken as the reference coordinates of the La, Nb, and O atoms.⁷ Decrease in the unit cell volume of complex oxides $\text{La}_{2/3-x}\text{Li}_{3x}\square_{4/3-2x}\text{Nb}_2\text{O}_6$ with increasing x takes place in accordance with the Vegard rule (Table 1) due to the substitution of lanthanum ions by lithium ions with smaller ionic radius ($R_{\text{La}}(\text{CN}=6) = 1.06 \text{ \AA}$, $R_{\text{Li}}(\text{CN}=6) = 0.74 \text{ \AA}$ ⁸). As follows from the table, substitution of lithium for lanthanum in solid solutions $\text{La}_{2/3-x}\text{Li}_{3x}\square_{4/3-2x}\text{Nb}_2\text{O}_6$ shifts the coordinates of the Nb, O₃, and O₄ atoms in the NbO_6 octahedron along the z axis (see Fig. 1). An analysis of the interatomic distances as a function of the amount of lithium (x) is illustrated in Fig. 2. The concentration dependences of the interatomic distances are characterized by a kink at $x = 0.17$. In the structure of $\text{La}_{2/3}\square_{4/3}\text{Nb}_2\text{O}_6$, the lanthanum atoms statistically occupy every other layer of cubooctahedra in the basic perovskite structure (positions 1a in Fig. 1).⁷ As a result of unsymmetrical electrostatic interaction (repulsion) between Nb atoms and the positive charge of the second coordination sphere, Nb atoms shift along the z axis towards the layer of “empty” 12-coordinated octahedra (cubooctahedra). It is obvious that when this layer is filled with cations (positions 1c in Fig. 1), Nb atoms will shift in the direction of 1a layer. This is observed in the structure of $\text{La}_{2/3-x}\text{Li}_{3x}\square_{4/3-2x}\text{Nb}_2\text{O}_6$ (Table, Fig. 2). It follows from Fig. 2 that as the amount of lithium (x) increases the Nb–O₁ interatomic distance decreases and the Nb–O₂ distance increases. This fact indicates that niobium atoms shift towards position 1a (Fig. 1) and

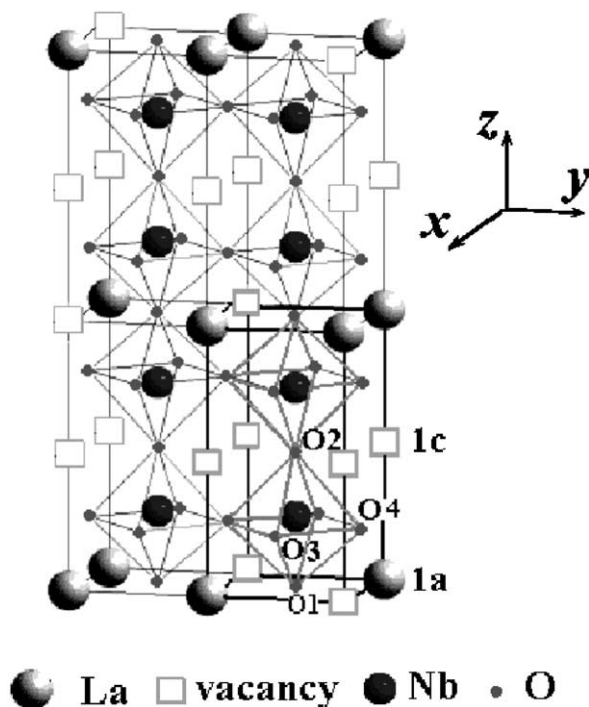


Fig. 1. Structure of defect perovskite $\text{La}_{2/3}\square_{4/3}\text{Nb}_2\text{O}_6$. Positions of atoms and vacancies: La (1a) 0 0 0; Nb (2t) $1/2 \ 1/2 \ z$; O₁ (1f) $1/2 \ 1/2 \ 0$; O₂ (1h) $1/2 \ 1/2 \ 1/2$; O₃ (2s) $1/2 \ 0 \ z$; O₄ (2r) $0 \ 1/2 \ z$; \square (1c) $0 \ 0 \ 1/2$.

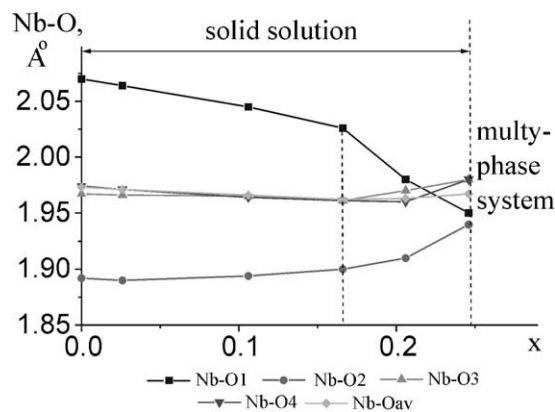


Fig. 2. Nb–O interatomic distances in the NbO_6 octahedron as a function of lithium content (x).

Table 1

Structure parameters of complex oxides in the system $\text{La}_{2/3-x}\text{Li}_{3x}\text{Nb}_2\text{O}_6$ as a function of lithium content (x)

Composition	$\text{La}_{0.64}\text{Li}_{0.08}\text{Nb}_2\text{O}_6$	$\text{La}_{0.56}\text{Li}_{0.32}\text{Nb}_2\text{O}_6$	$\text{La}_{0.5}\text{Li}_{0.5}\text{Nb}_2\text{O}_6$	$\text{La}_{0.46}\text{Li}_{0.62}\text{Nb}_2\text{O}_6$	$\text{La}_{0.42}\text{Li}_{0.74}\text{Nb}_2\text{O}_6$
<i>Unit cell parameters</i>					
a (Å)	3.9184(1)	3.906(2)	3.9002(1)	3.8948(1)	3.8943(1)
b (Å)	3.9086(1)	3.907(2)	3.9005(2)	3.9112(2)	3.900(1)
c (Å)	7.9081(2)	7.8785(2)	7.8521(2)	7.7936(5)	7.794(2)
V (Å ³)	121.115(6)	120.21(9)	119.452(6)	118.72(1)	118.38(5)
<i>Positions of atoms (z/c)</i>					
Nb	0.2610(2)	0.2596(2)	0.2580(2)	0.2545(4)	0.2503(7)
O ₃ /O ₄	0.234(1)	0.233(1)	0.232(1)	0.220(3)	0.208(4)
<i>Agreement factors</i>					
Rb (%)	7.14	8.39	9.14	9.57	15.1
Rf (%)	6.69	6.76	6.98	8.30	13.3
<i>Interatomic spacing Nb-O, Å</i>					
Nb-O ₁	2.064 (5)	2.045 (5)	2.026 (5)	1.98 (2)	1.95 (2)
Nb-O ₂	1.890(4)	1.894 (4)	1.900 (4)	1.91 (1)	1.94 (1)
Nb-O ₃ , ×2	1.966 (3)	1.965 (5)	1.961 (3)	1.97 (1)	1.98 (2)
Nb-O ₄ , ×2	1.971 (3)	1.964 (5)	1.961 (3)	1.96 (1)	1.98 (2)
(Nb-O)	1.971(4)	1.966(5)	1.962(4)	1.963(1)	1.967(2)
<i>Bottleneck size, S, Å²</i>					
l(a)↔l(a) ^a	14.48	14.31	14.17	13.25	12.42
l(a)↔l(c) ^b	15.32	15.26	15.21	15.23	15.19
l(c)↔l(c) ^c	16.44	16.39	16.37	16.89	17.51

^a $|\text{O}_1\text{-O}_1| \cdot |\text{O}_4\text{-O}_4| \cdot \sin\alpha_2$ ^b $|\text{O}_3\text{-O}_3| \cdot |\text{O}_4\text{-O}_4| \cdot \sin\alpha_3$ ^c $|\text{O}_2\text{-O}_2| \cdot |\text{O}_4\text{-O}_4| \cdot \sin\alpha_1$

reach symmetrical arrangement along the Z axis ($\text{Nb-O}_1 = \text{Nb-O}_2$) at $x \approx 0.25$. From these results it may be concluded that preferential occupation of positions 1a at $x = 0-0.5$ takes place at first. At $x > 0.5$, positions 1a are completely occupied, and positions 1c (vacancies) are occupied.

On the basis of the results of complex impedance at various lithium contents and temperatures, concentration dependences of the electrical conductivity (293–573 K) and activation energy of $\text{La}_{2/3-x}\text{Li}_{3x}\square_{4/3-2x}\text{Nb}_2\text{O}_6$ samples have been calculated. Isotherms of electrical conductivity against the amount of lithium are shown in Fig. 3. The activation energy of conductivity of the solid solution investigated is 0.32–0.48 eV for

samples with $x = 0-0.25$ (single-phase region) and 0.48–0.58 eV for samples with $x > 0.25$ (multiphase region), which corresponds to E_a of lithium-conducting solid electrolytes.

The increase in conductivity at room temperature to $\sigma \approx 10^{-4} \text{ S cm}^{-1}$ with increasing x ($x < 0.13$) is caused by an increase in current carrier concentration at a pretty large number of unoccupied vacancies ($[\square] = 1.08$). The decrease in conductivity and increase in activation energy in the range $x = 0.13-0.25$ (Figs. 3 and 4) is accounted for by a decrease in the number of vacant sites (at $x = 0.25$, $[\square] = 0.84$) and narrowing of migration channel (table) owing to the formation of substitutional solid solutions in this range, and at $x > 0.25$ also by the

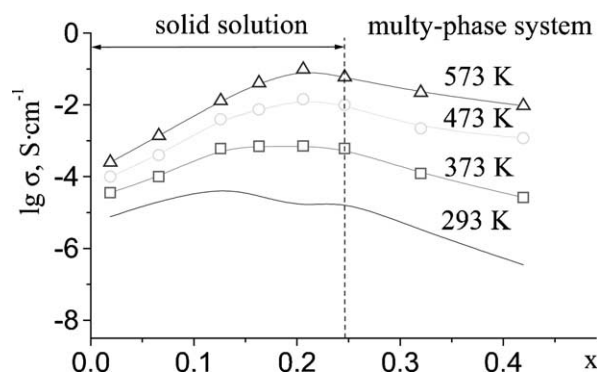


Fig. 3. Isotherms of electrical conductivity of $\text{La}_{2/3-x}\text{Li}_{3x}\square_{4/3-2x}\text{Nb}_2\text{O}_6$ samples as a function of lithium content (x).

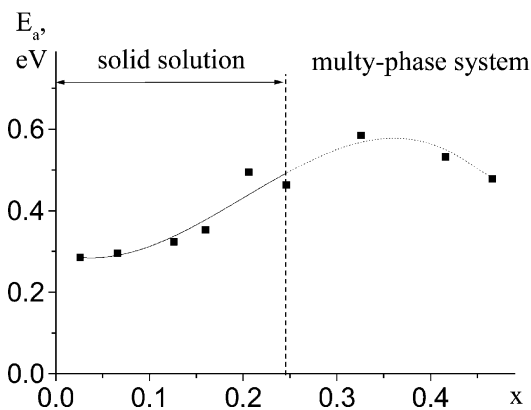


Fig. 4. Activation energy of conductivity (E_a) of $\text{La}_{2/3-x}\text{Li}_{3x}\square_{4/3-2x}\text{Nb}_2\text{O}_6$ samples as a function of lithium content (x).

contribution from the lithium-conducting phase LiNbO_3 with lower conductivity ($\sigma \approx 10^{-5} \text{ S cm}^{-1}$ at 293 K⁹).

The shift of the conductivity maximum σ_{max} towards higher x value and the considerable increase in σ_{max} ($\sigma_{\text{max}} \approx 10^{-3} \text{ S cm}^{-1}$ at 373 K, $\sigma_{\text{max}} \approx 10^{-1} \text{ S cm}^{-1}$ at 573 K) with increasing temperature are caused by an increase in the number of both charge carriers and thermally activated vacancies, which arises from an increase in lattice heat energy. At high temperature, migration channels, where ion transport takes place, widen, which also contributes to higher conductivity in the system.

The electrical conductivity of a material is known to be determined by concentration and mobility of charge carriers. One of the not unimportant factors that determine the ion mobility is the size of migration channels. Table 1 lists sizes S of the so-called “bottleneck”,¹⁰ between the adjacent positions $1a \leftrightarrow 1a$, $1a \leftrightarrow 1c$ and $1c \leftrightarrow 1c$ for lithium ion transport, which were calculated as the area of a parallelogram, which contains oxygen ions at the centers of each side. As x increases the S value between positions $1a \leftrightarrow 1c$ does not practically change, and between positions $1a \leftrightarrow 1a$ and $1c \leftrightarrow 1c$ it varies in a like manner to the concentration dependence of the Nb–O₁ and Nb–O₂ interatomic distances (Table 1, Fig. 2). For all compositions, the S value increases in the order: $1a \leftrightarrow 1a < 1a \leftrightarrow 1c < 1c \leftrightarrow 1c$ (Table 1). The mobility of cations is known to be determined by the optimum ratio of their size to that of migration channels.¹ As follows from the results presented in Table, migration channels may be both $1a \leftrightarrow 1c$ and $1c \leftrightarrow 1c$ directions. Investigation of interrelations between lithium ion mobility and migration channel size shows that ion transport in lithium-containing lanthanum titanate with defect-perovskite structure may take place at an interatomic distance more than 3.96 Å (i.e. Li–O = 1.99 Å).¹¹ Taking into account the above fact and the correlation between the concentration dependences of electrical conductivity (Fig. 3), activation energy (Fig. 4), and the “bottleneck” size in the direction $1c \leftrightarrow 1c$ (Table 1), it may be concluded that this direction is energetically a favorable pathway of lithium ion migration in $\text{La}_{2/3-x}\text{Li}_{3x}\square_{4/3-2x}\text{Nb}_2\text{O}_6$ oxides.

4. Conclusion

The homogeneity range of solid solutions $\text{La}_{2/3-x}\text{Li}_{3x}\square_{4/3-2x}\text{Nb}_2\text{O}_6$ with defect-perovskite structure

(rhombic distortion) at $x = 0\text{--}0.25$ has been determined, and structure parameters have been refined. It has been found that when Li^+ is substituted for La^{3+} in the structure of $\text{La}_{2/3}\square_{4/3}\text{Nb}_2\text{O}_6$, Nb atoms shift along the Z axis towards the layer of occupied cuboctahedra (position 1a) and reach symmetrical arrangement at $x = 0.25$.

It has been shown that in the structure of $\text{La}_{2/3-x}\text{Li}_{3x}\square_{4/3-2x}\text{Nb}_2\text{O}_6$, Li^+ cations occupy preferably positions 1a in the range $x = 0\text{--}\approx 0.5$, and occupy positions 1c (vacancies) at $x > 0.5$.

Transport properties of $\text{La}_{2/3-x}\text{Li}_{3x}\square_{4/3-2x}\text{Nb}_2\text{O}_6$ have been studied. It was noted that the direction $1c \leftrightarrow 1c$ is energetically a more favorable pathway of lithium ion migration.

It has been shown that materials with high lithium ion conductivity (at 573 K, $\sigma \approx 10^{-1} \text{ S cm}^{-1}$) can be produced on the basis of lithium-containing lanthanum metaniobates.

References

- Burmakin, Y. I., *Solid Electrolytes with Alkali-Cation Conduction (in Russian)*. Nauka, Moscow, 1992.
- Belous, A. G., Novitskaya, G. N., Polyanetskaya, S. V. and Gornikov, Y. I., Investigation of complex oxides of the composition $\text{La}_{2/3-x}\text{Li}_{3x}\text{TiO}_3$. *Izvestiya AN SSSR, Neorgan. Mater.*, 1987, **23**, 470–472.
- Yyer, P. N. and Smith, A. I., Double oxides containing niobium, tantalum or protoactinium. III. Systems involving the rare-earth. *Acta Crystallogr.*, 1967, **23**, 740–746.
- Certificate of Analysis. Standard Reference Material 1976, Instrument Sensitivity Standard for X-ray Powder Diffraction*. National Institute of Standards & Technology, Gaithersburg, 1991.
- Torii, Y., Schiye, T. and Yamamoto, T., Crystallization of rapid quenching of $\text{La}_{0.33}\text{NbO}_3$ melt. *Mater. Res. Bull.*, 1982, **17**, 727.
- Nalbandyan, V. B. and Shukaev, I. A., Novel tantalates and niobates. *Zhurn. Neorg. Khim.*, 1989, **34**, 793–795.
- Trunov, V. K., Yevdokimov, A. A., Frolov, A. M. and Averina, I. M., Refinement of the structure of $\text{La}_{0.33}\text{NbO}_3$. *Kristallografiya*, 1981, **26**, 189–191.
- Shannon, R. D. and Riewitt, C. T., Effective ionic radii in oxides and fluorides. *Acta Cryst.*, 1969, **25B**, 925–946.
- Glass, A. M., Nassau, K. and Negran, T. J., Ionic conductivity of quenched alkali niobate and tantalite. *J. Appl. Phys.*, 1978, **49**, 4808–4812.
- Latie, L., Villeneuve, G., Conte, D. and Le Flem, G., Ionic conductivity of oxides with general formula $\text{Li}_x\text{Ln}_{1/3}\text{Nb}_{1-x}\text{Ti}_x\text{O}_3$ (Ln = Nd, Nd). *J. Sol. State Chem.*, 1984, **51**, 293–299.
- Paris, M. A., Sanz, J., Leon, C., Ibarra, J. and Varez, A., Li Mobility in the orthorhombic $\text{Li}_{0.18}\text{La}_{0.61}\text{TiO}_3$ Perovskite Studied by NMR and Impedance Spectroscopies. *Chem. Mater.*, 2000, **12**, 1694–1701.